Unstructured Finite Volume Computational Thermo-Fluid Dynamic Method for Multi-Disciplinary Analysis and Design Optimization

Alok Majumdar & Paul Schallhorn
Sverdrup Technology, Inc.
Huntsville, Alabama 35806

IN-77
372 717

Abstract

This paper describes a finite volume computational thermo-fluid dynamics method to solve for Navier-Stokes equations in conjunction with energy equation and thermodynamic equation of state in an unstructured coordinate system. The system of equations have been solved by a simultaneous Newton-Raphson method and compared with several benchmark solutions. Excellent agreements have been obtained in each case and the method has been found to be significantly faster than conventional Computational Fluid Dynamic(CFD) methods and therefore has the potential for implementation in Multi-Disciplinary analysis and design optimization in fluid and thermal systems. The paper also describes an algorithm of design optimization based on Newton-Raphson method which has been recently tested in a turbomachinery application.

Nomenclature

Symbol	Description
A	Area (in^2)
C_L	Flow Coefficient
d, D	Diameter (in)
g	Gravitational Acceleration (ft/sec^2)
g_c	Conversion Constant (= 32.174 $lb\text{-}ft/lb_f\text{-}sec^2$)
K_f	Flow Resistance Coefficient ($/lb_f\text{-}sec^2/(lb\text{-}ft)^2$)
K_{rot}	Non-dimensional Rotating Flow Resistance Coefficient
L	Length (in)
$\dot{m}$	Mass Flow Rate (lb/sec)
p	Pressure (lb_f/in^2)
Re	Reynolds Number ($Re = \rho uD/\mu$)
r	Radius (in)
S	Momentum Source (lb_f)
T	Temperature (^{o} F)
u, v	Velocity (ft/sec)
x	Coordinate Direction (in), Quality
y	Coordinate Direction

Greek

ρ	Density (lb/ft^3)
θ	Angle Between Branch Flow Velocity Vector and Gravity Vector (deg), Angle Between Neighboring Branches for Computing Shear (deg)
ω	Angular Velocity (rad/sec)
ε	Absolute Roughness (in)
ε/D	Relative Roughness
μ	Viscosity (lb/ft-sec)

1.0 Introduction

Computational fluid dynamic methods have been extensively used to analyze a new design or to investigate operational problems in Aerospace, Automobile, Nuclear and Process Industries. Finite volume method [1] has been the most popular among the available method to solve for multi-dimensional Navier-Stokes equations. Several commercial CFD codes [2-6] are based on finite volume method. Most CFD models require extensive computer resources to perform a single analysis. For example a typical flow calculation in a compressor blade requires several hours in a supercomputer and typical turnaround time is one week. Although there was a need, Multi-disciplinary analysis and design optimization for fluid and thermal systems have not been found very practical in industries.

The SIMPLE (Semi-Implicit Pressure Linked Equation) algorithm [7] has been widely used in all finite volume based computer codes mentioned earlier. Although there are several improvements to the original algorithm, SIMPLE is still based on successive substitution method. Momentum and continuity equations are solved separately. A pressure correction equation is derived from continuity equation using a linearized momentum equation. Under-relaxation is often necessary to ensure convergence. It slows down computational speed significantly. On the other hand simultaneous solution of all governing equations eliminates the need for under-relaxation and convergence is obtained much faster than any method using a successive substitution technique. Moreover, most commercially available computer codes use a structured coordinate system to define the flow configuration. In industrial applications majority of the flow situations can not be easily modeled using a structured coordinate system. Therefore a need exists for an efficient numerical algorithm for solving Navier-Stokes equation in an unstructured co-ordinate system which can be utilized for multi-disciplinary design optimization and analysis. The purpose of this paper is to describe the extension of the Generalized Fluid System Simulation Program (GFSSP) [8], a network flow analysis code to account for multidimensional flow effects. GFSSP discretizes an irregular flow domain in nodes and branches. The scalar transport equations such as mass and energy conservation equations are solved at the nodes where as the vector properties such as momentum are solved in branches. GFSSP has been extensively applied in propulsive flows [9-10] and it demonstrated a satisfactory numerical stability in wide range of flow situations. In this paper an attempt has been made to extend GFSSP's solver to handle multi-dimensional flow and demonstrate its use for a design problem.

2.0 Unstructured Finite Volume Grid

The unstructured finite volume grid network for GFSSP is shown in Figure 1, which shows connectivity of five nodes with four branches. In this figure node-i is connected with four neighboring nodes (J = 1 to 4) . In structured coordinate systems the number of neighboring nodes are restricted to 2, 4 and 6 for one, two and three dimensional systems

respectively. On the other hand for an unstructured system, there is no such restriction on the number of neighboring nodes. The index k represents fluid species.

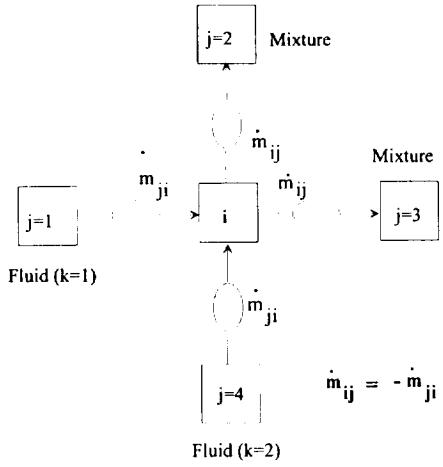

Figure 1: Schematic of Nodes and Branches for an Unstructured Finite Volume Grid

3.0 Conservation Equations

3.1 Mass Conservation Equation

The mass conservation equation for the ith node can be represented by:

$$\sum_{j=1}^{n} \dot{m}_{ij} = 0 \qquad (1)$$

Equation 1 implies that the net mass flow from a given node must equate to zero. In other words, the total mass flow rate into a node is equal to the total mass flow rate out of the node.

3.2 Momentum Conservation Equation

The one dimensional form of momentum equation for every branch takes the following form:

$$\frac{\dot{m}_{ij}}{g_c}\left(u_i - u_u\right) = \left(p_i - p_j\right)A + \frac{\rho\, g V \cos\theta}{g_c} - K_f \dot{m}_{ij}\left|\dot{m}_{ij}\right| A + \frac{\rho\, K_{rot}^2 \omega^2 A}{2\, g_c}\left(r_j^2 - r_i^2\right) + S \qquad (2)$$

Inertia Pressure Gravity Friction Centrifugal Source

Equation 2 represents the balance of fluid forces acting on a given branch. Inertia, pressure, gravity, friction and centrifugal forces are considered in the conservation equation. In addition to five forces, a source term S has been provided in the equation to

input pump characteristics or to input power to pump in a given branch. If a pump is located in a given branch, all other forces except pressure are set to zero. The source term S is set to zero in all other cases. Figure 2 shows the schematic of a branch control volume.

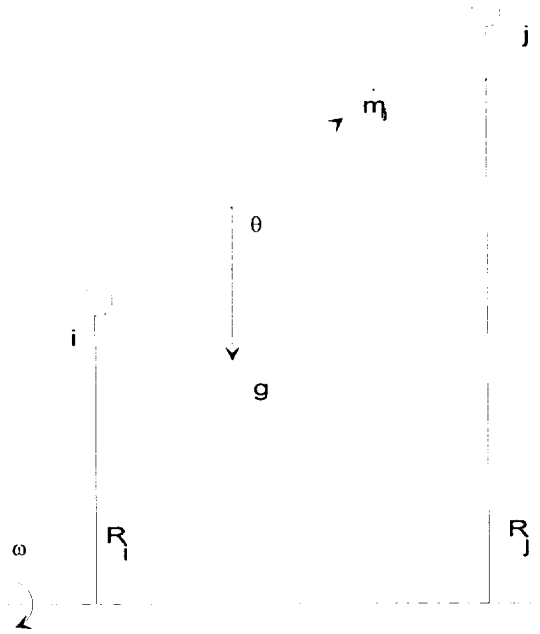

Figure 2: Schematic of a Branch Control Volume Showing the Gravity and Rotation

Multi-dimensional conservation equations must account for the transport of mass, momentum and energy into and out of the control volume from all directions in space. Mass conservation equations (Equation 1) can account for such transport because each internal node can be connected with multiple neighboring nodes located in space in any arbitrary location (Figure 1). On the other hand, the momentum conservation equation (Equation 2) is one dimensional. Multi-dimensional momentum transport can be accounted for by incorporating two additional terms in the momentum equation. These terms include: a) momentum transport due to shear, and b) momentum transport due to the transverse component of velocity.

These two terms can be identified in the two-dimensional steady state Navier-Stokes equation which can be expressed as:

$$\rho\left(u\frac{\partial u}{\partial x}+v\frac{\partial u}{\partial y}\right) = \frac{\partial(\rho uu)}{\partial x}+\frac{\partial(\rho vu)}{\partial y} = -\frac{\partial p}{\partial x}+\rho g_x+\mu\left(\frac{\partial^2 u}{\partial x^2}+\frac{\partial^2 u}{\partial y^2}\right) \qquad (3)$$

The first term on the left hand side of Equation 3 corresponds to the current inertia term described in Equation 2 . The second term on the left hand side of Equation 3 corresponds to the transverse momentum exchange. The first term on the right hand side

corresponds to the pressure term in Equation 2. The second term on the right hand side of Equation 3 corresponds to the gravity term. The third term on the right hand side of the equation is negligible (based on an order of magnitude argument). The fourth term on the right hand side represents momentum transport due to shear. This section discusses the implementation of shear and transverse momentum transport into the momentum equation of GFSSP.

3.3 Momentum Transport Due to Shear

Begin by examining the shear term (fourth term) of the Navier-Stokes Equation in more detail. First, consider the shear as a force instead of a force per unit volume by multiplying the volume by the shear term.

$$\mu \frac{\partial^2 u}{\partial y^2} V \approx \mu \frac{\Delta u}{(\Delta y)^2} (\Delta x)(\Delta y)(\Delta z) = \mu \frac{\Delta u}{\Delta y} \Delta x \Delta z = \mu \frac{\Delta u}{\Delta y} A_{shear} \qquad (4)$$

Figure 3 represents a set of nodes and branches for which shear forces are exchanged. Let branch 12 represent the branch for which the shear force is to be calculated. Branches N12 and S12 represent the parallel branches which will be used to calculate the shear force on branch 12. Let YS be the distance between branches 12 and S12, and let YN be the distance between branches 12 and N12. Let AS be the shearing area between branches 12 and S12, while AN is the shearing area between branches 12 and N12.

A differencing scheme that can account for non-orthogonality in node structure was used. Equation 5 represents the shear term for branch 12. The angle θ represents the angle that adjacent branches make with respect to the referenced branch.

$$\mu \frac{\partial u}{\partial y} A_{Branch\ 12\ shear} \approx \left[\left(\mu \frac{u_{N12} \cos\theta_{N12} - u_{12}}{YN} AN \right) + \left(\mu \frac{u_{12} - u_{S12} \cos\theta_{S12}}{YS} AS \right) \right] \qquad (5)$$

Equation 5 can be generalized to n-number of parallel branches at any position around branch 12 as shown in Equation 6.

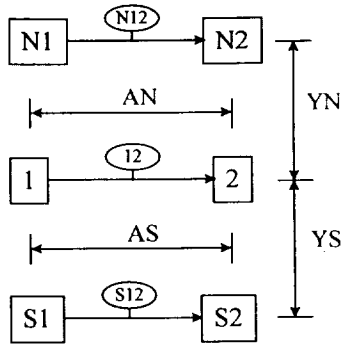

Figure 3: Branch and Node Schematic for Shear Exchange

$$\mu \frac{\partial u}{\partial y} A_{\text{Branch 12 shear}} \approx \sum_{i=1}^{n} \left(\mu \frac{u_{i12} \cos\theta_{i12} - u_{12}}{Yi} Ai \right) \tag{6}$$

Where the summation subscript i represents the i^{th} parallel branch to branch 12.

Next, the shear interaction with a neighboring parallel wall should be addressed. Suppose that adjacent to branch 12 is a wall that is approximately parallel to the branch. The angle θ_{wall} represents the angle between branch 12 and the wall. The wall has a velocity v_{solid}. The distance between the centerline of branch 12 and the wall is y_{wall} and the shear area is A_{wall}. The expression for the shear effect of the wall on branch 12 is given in Equation 7.

$$\mu \frac{\partial u}{\partial y} A \Big|_{\text{Branch 12 -wall}_{\text{shear}}} \approx \mu \frac{u_{wall} \cos\theta_{wall} - u_{12}}{y_{wall}} A_{wall} \tag{7}$$

If there were multiple walls adjacent to branch 12, then Equation 7 could be generalized into Equation 8.

$$\mu \frac{\partial u}{\partial y} A \Big|_{\text{Branch 12 -wall}_{\text{shear}}} \approx \sum_{i=1}^{n} \left(\mu \frac{u_{wall_i} \cos\theta_{wall_i} - u_{12}}{y_{wall_i}} A_{wall_i} \right) \tag{8}$$

Finally, combining the adjacent branch and the wall shear equations into one generalized equation for the i^{th} branch for which shear is to be calculated. Equation 9 represents the actual laminar shear formulation incorporated into GFSSP, where i is the current branch, np_i is the number of parallel branches to branch i, and ns_i is the number of parallel solid walls to branch i.

$$\mu \frac{\partial u}{\partial y} A_{\text{Branch i shear}} \approx \sum_{j=1}^{np_i} \left(\mu \frac{u_{ij} \cos\theta_{ij} - u_i}{Y_{ij}} A_{ij} \right) + \sum_{k=1}^{ns_i} \left(\mu \frac{u_{wall\,ik} \cos\theta_{wall\,ik} - u_i}{y_{wall\,ik}} A_{ik} \right) \tag{9}$$

3.4 Transverse Momentum Transport

The transverse momentum component of Equation 3 can be expressed in terms of a force per unit volume.

$$\frac{\partial \rho v u}{\partial y} V \approx \frac{(\rho v \Delta u)}{(\Delta y)} (\Delta x)(\Delta y)(\Delta z) = (\Delta x)(\Delta z)(\rho v \Delta u) = \dot{m}_{trans} \Delta u \qquad (10)$$

Figure 4 represents a set of nodes and branches for which transverse momentum exchange will take place. Let the branch 12 represent the current branch which will receive transverse momentum from the surrounding branches. Branch S12 represents an adjacent parallel branch, while branches S1 and S2 represent the adjacent normal branches.

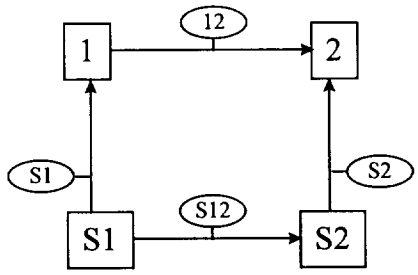

Figure 4: Branch and Node Schematic for Transverse Momentum Exchange

Now, examine the formulation for calculating the transverse momentum term for branch 12. First, calculate the average mass flow rate for the adjacent normal branches:

$$\dot{m}_S = \frac{1}{2}\left(\dot{m}_{S1} + \dot{m}_{S2}\right) \qquad (11)$$

Examining Figure 4, a positive transverse mass flow rate is defined as flow into the nodes corresponding to the branch in question. Based on this definition of transverse mass flow rate, calculate the transverse momentum term:

$$\left.\frac{\partial \rho v u}{\partial y} V\right|_{12} \approx \left(\dot{m}_S u_{12} - \dot{m}_S u_{S12}\right) = \dot{m}_S \left(u_{12} - u_{S12}\right) \qquad (12)$$

The parallel branch (S12) will contribute to the transverse momentum term of branch 12 when $\dot{m}_{12} \geq 0$ (since a positive transverse flow rate begins at S12 and ends at 12), and should have a negligible contribution when $\dot{m}_{12} < 0$ (i.e. transverse flow rate begins at 12

and ends at S12). Equation 13, below, is the upwinding representation of the transverse momentum term for branch 12.

$$\left.\frac{\partial \rho v u}{\partial y} V\right|_{12} \approx u_{12}\left(\max\left\|-\dot{m}_S, 0\right\|\right) - u_{S12}\left(\max\left\|0, \dot{m}_S\right\|\right) \tag{13}$$

Equation 13 can be generalized for m-parallel branches around branch i, each with an angle θ_{ij} with respect to branch i, and n_{ij} corresponding transverse connecting branches, each transverse branch with an angle of θ_{ijk} with respect to branch i. Equation 14 represents this generalized version of Equation 13.

$$\left.\frac{\partial \rho v u}{\partial y} V\right|_i \approx \sum_{j=1}^{m_i}\left[u_i\left(\max\left\|-\sum_{k=1}^{n_{ij}}\left\{\frac{1}{n_{ij}}\dot{m}_{ijk}\cos\theta_{ijk}\right\}, 0\right\|\right) - \left(u_{ij}\cos\theta_{ij}\right)\left(\max\left\|0, \sum_{k=1}^{n_{ij}}\left\{\frac{1}{n_{ij}}\dot{m}_{ijk}\cos\theta_{ijk}\right\}\right\|\right)\right] \tag{14}$$

Equation 14 represents the actual transverse momentum formulation put into GFSSP, where i is the current branch for which transverse momentum is being calculated, m_i is the number of parallel branches which will be used to calculate transverse momentum, and n_{ij} is the number of connecting transverse branches between the current branch (i), and the j^{th} parallel branch.

4.0 Verification Results

In order to verify proper implementation of the shear and transverse momentum components into GFSSP, two models were identified and developed. The two verification models are: two dimensional Poiseuille flow and two dimensional shear driven flow in a square cavity. The following sections describe the models and present the results.

4.1 Poiseuille Flow Model

Consider the flow between two fixed flat plates shown below in Figure 5. The flow is pressure driven and assumed to be fully developed. The length of the plates is 1000 inches, they are 1 inch apart, the fluid density is 12 lb_m/ft^3, the viscosity is 1 $lb_m/(ft \cdot sec)$, and the pressures at the upstream and downstream ends are 20 psi and 10 psi, respectively. The analytical solution (Equation 15) for this situation can easily be derived for laminar flow, and is provided below for comparative purposes. Figure 6 shows an approximate velocity profile for this situation.

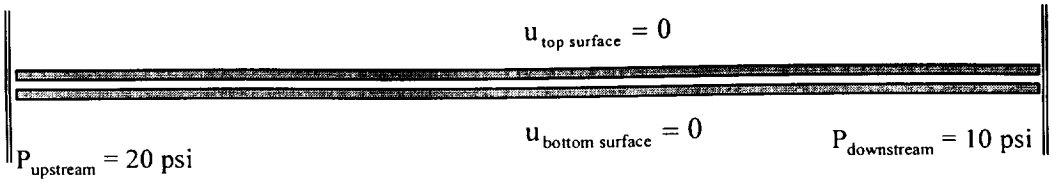

Figure 5: Poiseulle Flow Physical Situation

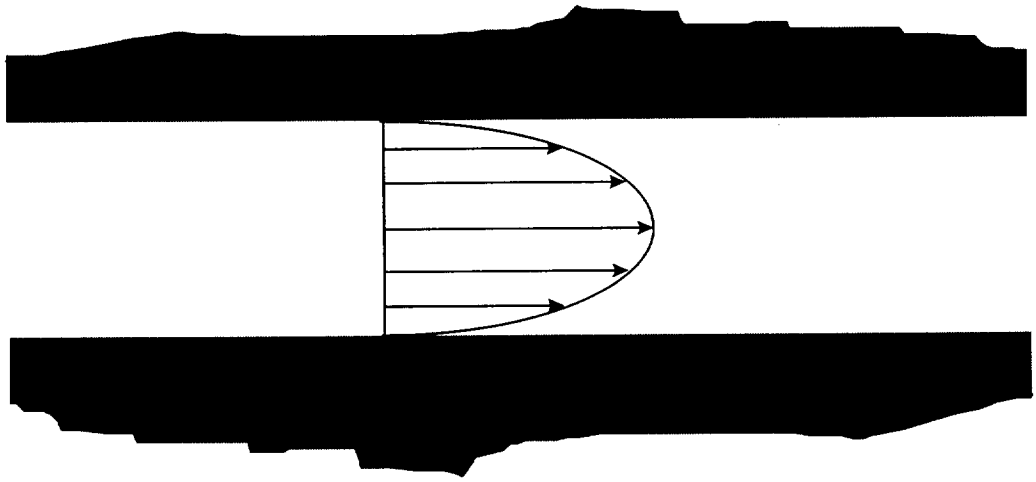

Figure 6: Poiseulle Flow Velocity Profile

$$u = 0.005(y - y^2) \tag{18}$$

A simple 3 node, 10 branch model (two sets of 5 parallel branches) was constructed to model the physical situation described above. The model is shown schematically in Figure 7.

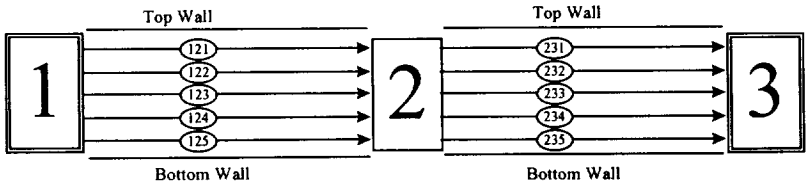

Figure 7: GFSSP Poiseulle Flow Model

Each of the 10 branches (121-125, 231-235) are 500 inches in length. It is assumed that the shear area for each branch-branch & branch-wall was 500 in^2 and that the shear distance was 0.2 inches between adjacent branches and 0.1 inch between walls and their adjacent branches. The pressures at nodes 1 and 3 are 20 psi and 10 psi, respectively. A constant density option was used and the corresponding density and viscosity used were $12 lb_m/ft^3$ and 1.0 $lb_m/(ft\cdot sec)$, respectively. Resistance option -02 was used in the initial

flow field calculation (for the first Newton-Raphson iteration, after which the shear will replace the friction factor calculation) for each of the branches. The bottom and top walls are fixed.

Figure 8 below shows a comparison between the velocity profiles for the analytical solution and the GFSSP 3 node, 10 branch (5 parallel branch) model. As can be seen in Figure 8, the results of this crude GFSSP model compare vary favorably with the analytical solution.

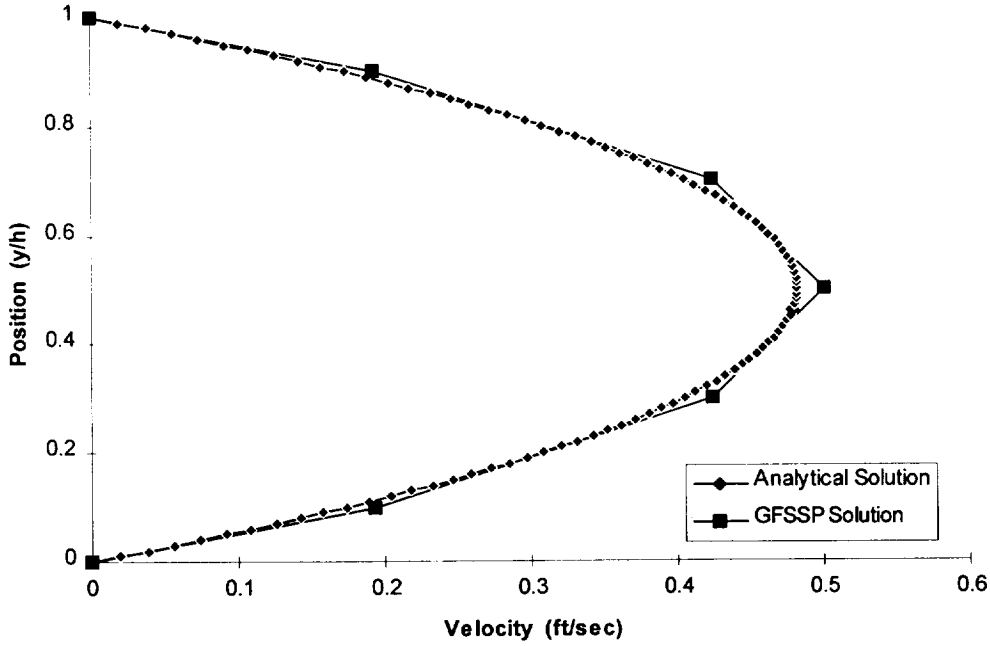

Figure 8: Poiseulle Flow Velocity Distribution

4.2 Shear Driven Flow in a Square Cavity

Consider a square cavity as shown below in Figure 9. The flow is induced by shear interaction at the top wall. The length of each wall is 12 inches. The density of the fluid is assumed constant at 1.00 lb_m/ft^3, and the viscosity of the fluid is assumed to be 1.00 $lb_m/(ft\,sec)$. The bottom and side walls are fixed. The top wall is moving to the right at constant speed of 100 ft/sec. The corresponding Reynolds number for this situation is Re = 100.

4.2.1 Benchmark Numerical Solution

Due to the non-linearity of the governing differential equations, an analytical solution of this situation is not available. Instead of an analytical solution, a well known numerical solution by Odus Burggraf [9] was used as the benchmark solution. Burggraf used a 51x51 grid in his model of the square cavity.

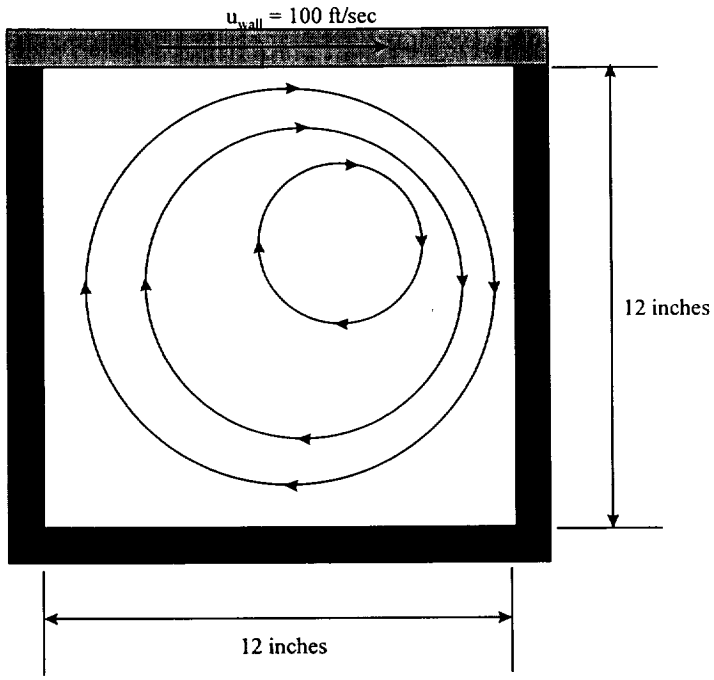

Figure 9: Flow in a Shear Driven Square Cavity

4.2.2 GFSSP Driven Cavity Model

The GFSSP model of the driven cavity consists of 49 nodes (48 of which are internal) and 84 branches. For numerical stability, one node (Node 1) was assigned to be a boundary node with an arbitrary pressure of 100 psi. A unit depth (1 inch) was assumed for the required areas. The model is shown schematically in Figure 10.

It was assumed that the shear area for each branch is 2.0 in^2. The shear distance between adjacent branches is 1.71429 inches and the shear distance between walls and their adjacent branches is 0.85714 inches. For transverse momentum, only adjacent parallel branches were considered, and only connecting branches not associated with the boundary node were used. A constant density option was used with corresponding density and viscosity values of 1.0 lb_m/ft^3 and 1.0 $lb_m/(ft\,sec)$, respectively. Resistance Option 2 was used in the initial flow field calculation (for the first Newton-Raphson iteration, after which the shear will replace the friction factor calculation) for all of the

branches. The bottom and side walls are fixed. The top walls are moving to the right at 100 ft/sec. All parallel angles are 0°, and all transverse angles are 90°.

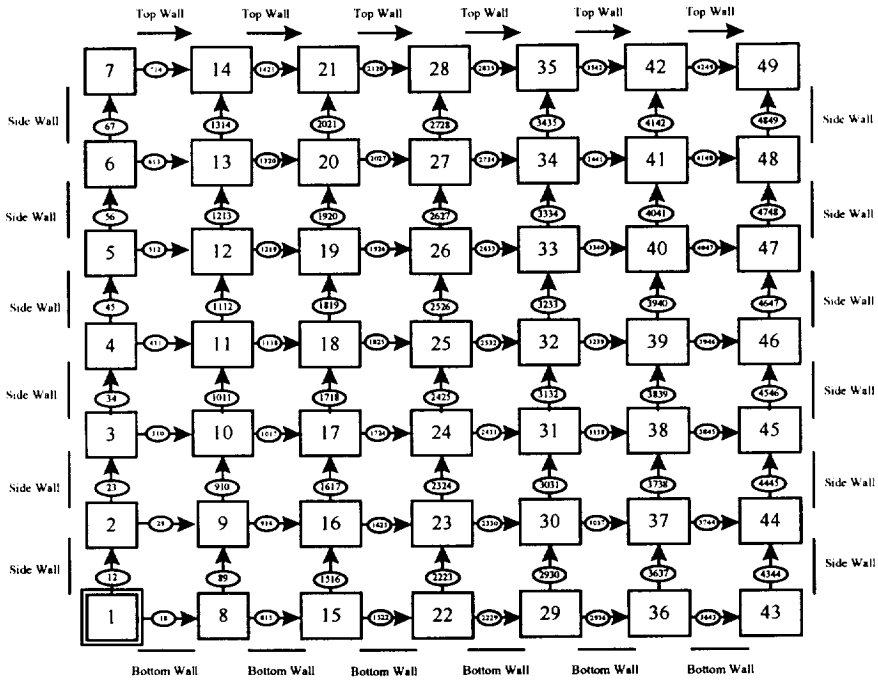

Figure 10: GFSSP Flow in a Shear Driven Square Cavity Model

4.2.3 Results

Figure 11 shows a comparison between the benchmark numerical solution and GFSSP 7x7 node model velocity profiles along a vertical plane at the horizontal midpoint. As can be seen in Figure 11, the results of this crude GFSSP model compare very favorably with the benchmark numerical solution of Burggraf [11].

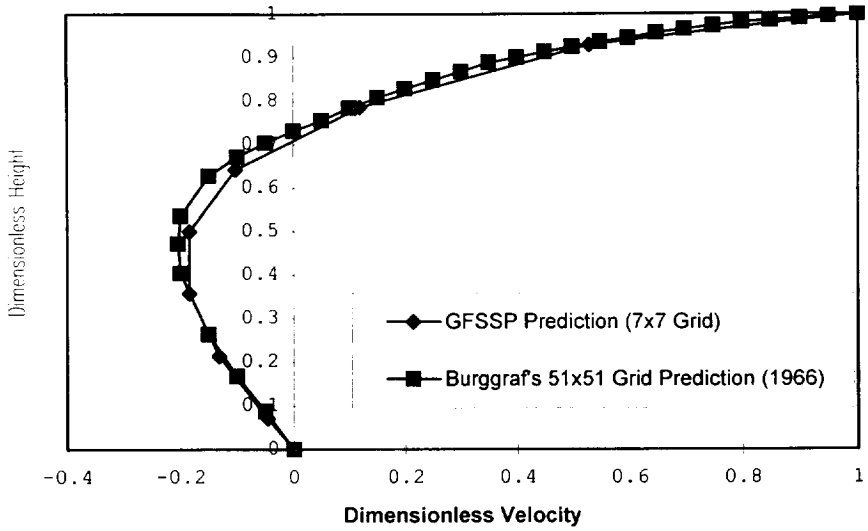

Figure 11: Shear Driven Square Cavity Centerline Velocity Distribution

5.0 Design Mode

The design of a system is an iterative process, and all iterative schemes follow a 'guess and correct' procedure. With an intelligent guess one can reduce the required number of iterations and therefore can reduce the cost of the design of such system. In the past, every engineering organization depended on a few experienced engineers who can make such intelligent guesses by virtue of their long years of experience in a particular discipline. Because of the changing nature of the economy and technological developments, availability of such precious human resources are in decline. The future design of engineering hardware will be based on a computer based iterative process where an intelligent guess will no longer contribute to the economic aspect of the design. All design decisions will be based on computer models.

5.1 Overview of the Design Mode Methodology

This section describes how GFSSP's analysis capability can be utilized for designing a fluid system. Suppose we want to specify a number of design variables in the flow circuit. These variables could be a) pressure at a given node(p_n), b) flow rate in a particular branch(m_b) and c) temperature at a given node(T_n). It is necessary to identify the parameters that can be adjusted to attain the desired variables. Let us suppose these parameters are a) area of a particular branch, A_x, b) Pressure at a given boundary node, p_x, and c) Heat load at a given node, Q_x. It should be noted that the number of desired variables must be equal to the number of identified parameters that can be adjusted during the iterative scheme.

Following are the seven steps of Newton-Raphson method proposed for design mode calculation:
The application of the Newton-Raphson Method involves the following 7 steps:

1. Develop the governing equations.

The equations are expressed in the following form:

$$F_1(p_n, A_x, p_x, Q_x) = p_n - f(A_x, p_x, Q_x) = 0$$
$$F_2(m_b, A_x, p_x, Q_x) = m_b - f(A_x, p_x, Q_x) = 0 \qquad (16)$$
$$F_3(T_n, A_x, p_x, Q_x) = m_b - f(A_x, p_x, Q_x) = 0$$

2. Guess a solution for the equations.

Guess A^*_x, p^*_x, Q^*_x as an initial solution for the governing equations

3. Calculate the residuals of each equation.

When the guessed solutions are substituted into Equation 16, the right hand side of the equation is not zero. The non-zero value is the residual.

$$F_1(p_n, A^*_x, p^*_x, Q^*_x) = p_n - f\ (\ A^*_x, p^*_x, Q^*_x) = R_1$$
$$F_2(m_b, A^*_x, p^*_x, Q^*_x) = m_b - f\ (\ A^*_x, p^*_x, Q^*_x) = R_2 \qquad (17)$$
$$F_3(T_n, A^*_x, p^*_x, Q^*_x) = T_n - f\ (\ A^*_x, p^*_x, Q^*_x) = R_3$$

The intent of the solution scheme is to correct A^*_x, p^*_x, Q^*_x with a set of corrections A'_x, p'_x, Q'_x such that R_1, R_2, R_3 are zero.

4. Develop a set of correction equations for all variables.

First construct the matrix of influence coefficients:

$$\begin{matrix} \frac{\partial F_1}{\partial A_x} & \frac{\partial F_1}{\partial p_x} & \frac{\partial F_1}{\partial Q_x} \\ \frac{\partial F_2}{\partial A_x} & \frac{\partial F_2}{\partial p_x} & \frac{\partial F_2}{\partial Q_x} \\ \frac{\partial F_3}{\partial A_x} & \frac{\partial F_3}{\partial p_x} & \frac{\partial F_3}{\partial Q_x} \end{matrix} \tag{18}$$

Then construct the set of simultaneous equations for corrections:

$$\begin{bmatrix} \frac{\partial F_1}{\partial A_x} & \frac{\partial F_1}{\partial p_x} & \frac{\partial F_1}{\partial Q_x} \\ \frac{\partial F_2}{\partial A_x} & \frac{\partial F_2}{\partial p_x} & \frac{\partial F_2}{\partial Q_x} \\ \frac{\partial F_3}{\partial A_x} & \frac{\partial F_3}{\partial p_x} & \frac{\partial F_3}{\partial Q_x} \end{bmatrix} \begin{bmatrix} A_x' \\ p_x' \\ Q_x' \end{bmatrix} = \begin{bmatrix} R_1 \\ R_2 \\ R_3 \end{bmatrix} \tag{19}$$

5. Solve for A_x', p_x', Q_x' by solving the simultaneous equations.

6. Apply correction to each variable.

7. Iterate until the corrections become very small.

5.2 An Example of the Design Mode Methodology

5.2.1 Description

It is required to estimate the cross-sectional area of a pressure regulator to set the downstream pressure at 55 psia. The pressure regulator is located 25" downstream in a (1/4" OD, 0.18" ID) pipeline with a relative roughness of 0.00006. The pipeline is connected with a 300 psia, 70° F nitrogen supply line. Nitrogen is vented to the atmosphere at 14.7 psia and 70° F at 60" downstream of the pressure regulator. The diameters and roughness are identical for both pipes. A flow restriction with a loss coefficient (C_L) of 0.6 is used to model the pressure regulator. Figure 12 schematically shows the situation to be modeled.

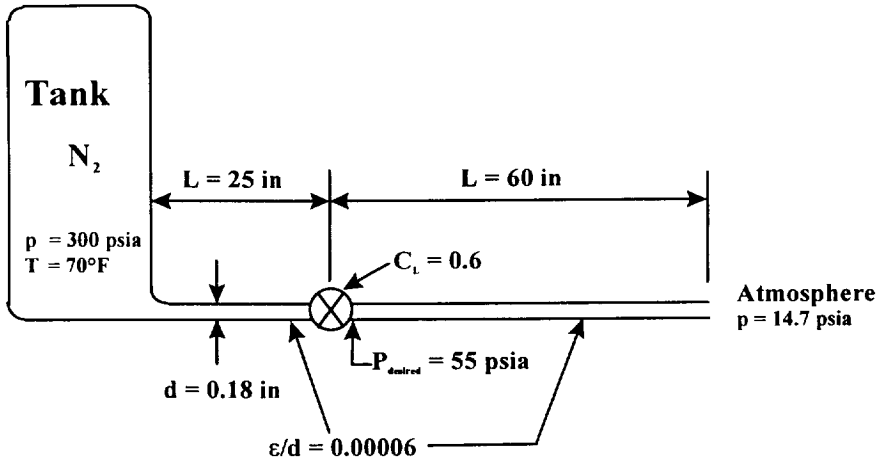

Figure 12: Schematic of the Pressure Regulator System to be Modeled

5.2.2 GFSSP Model

The GFSSP model used to predict the pressure downstream of the pressure regulator is shown in Figure 13. Node 1 represents the tank, node 2 represents a position just upstream of the pressure regulator, node 3 represents a position just downstream of the regulator, and node 4 represents the atmosphere. Branch 23 represents the regulator, whereas branches 12 and 34 represent the pipes up- and downstream of the regulator. An initial guess of the cross-sectional area of the pressure regulator is made and a predicted pressure downstream of the regulator is calculated, which is likely to be different from the desired pressure of 55 psia. The intent of this exercise is to adjust the area until the desired pressure is achieved. The Design Mode Methodology, described in Section 5.1, is used adjust the regulator area within a convergence criterion of 0.01 on the desired pressure.

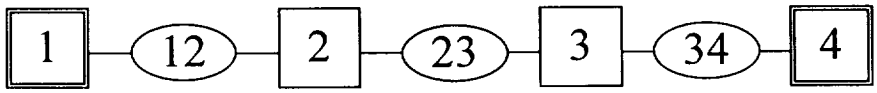

Figure 13: GFSSP Model of the Pressure Regulator System

5.2.3 Results

An initial guess of the pressure regulator cross-sectional area was made of 0.002 inches. Using this area, GFSSP predicted the pressure at node 3 to be 27.2 psia (well below the desired pressure of 55 psia). The Design Mode methodology, described in section 5.1, was employed to predict a new area for branch 23, and then a new predicted pressure was calculated for node 3. This process was repeated until the convergence criteria was met (three iterations were required). Table 1 summarizes the cycle of guessed and predicted values.

Table 1: Summary of Guessed and Predicted values for Design Mode Example

Iteration	A_{23} Guessed (in^2)	P_3 Predicted (psia)	Converged?	A_{23} New (in^2)
1	0.002	27.20	N	0.005658
2	0.005658	54.71	N	0.0057
3	0.0057	55.00	Y	

This systematic iterative procedure to adjust certain variables to achieve a design goal has also been demonstrated [12] in a turbomachinery application.

6.0 Conclusions

A finite volume based network analysis method was extended to perform multi-dimensional flow calculations in an unstructured co-ordinate system. Two classical flow problems were solved and results compared very well with benchmark analytical and numerical solution. Simultaneous solution of mass and momentum conservation equations was found more economical than conventional successive substitution employed in conventional CFD methods. The simultaneous method of solving Navier-Stokes equation make it more feasible to apply for multi-disciplinary analysis and design optimization. A design algorithm based on Newton-Raphson method was described and a simple application of the design method was demonstrated by solving a problem of finding the required area of a pressure regulator in a compressible flow feed line.

7.0 References

1. Patankar, S. V., "Numerical Heat Transfer and Fluid Flow", Hemisphere Publishing Corp., Washington, D. C., 1980.
2. PHOENICS - A general purpose CFD code developed by CHAM of North America, London, UK.
3. FLUENT - A general purpose CFD code developed by Fluent Inc, Lebanon, New Hampshire.
4. CFX - A general purpose CFD code developed by AEA Technology, Pittsburgh, Pennsylvania.
5. CFD-ACE - A general purpose CFD code developed by CFDRC, Huntsville, Alabama.
6. MICROCOMPACT - A general purpose CFD code developed by Innovative Research, Minneapolis, Minnesota.
7. Patankar, S. V. and Spalding, D. B., "A Calculation Procedure for Heat, Mass and Momentum Transfer in three-dimensional Parabolic Flows" Int. J. Heat Mass Transfer, vol. 15, 1972, p. 1787

8. Majumdar, A. K.: "A Generalized Fluid System Simulation Program to Model Flow Distribution in Fluid Networks," Sverdrup Technology Report No. 331-201-96-003, October 1996.
9. Majumdar, A. K. and VanHooser, K. P., "A General Fluid System Simulation Program to Model Secondary Flows in Turbomachinery", Paper No. AIAA 95-2969, 31st AIAA/ASME/SAE/ASEE Joint Propulsion Conference, July 10-12, 1995, San Diego, California.
10. Majumdar, A. K., Bailey, J. W., Holt, K. A. and Turner, S. G., "Mathematical Modeling of Free Convective Flows for Evaluating Propellant Conditioning Concepts", Paper No. AIAA 96-3117, 32nd AIAA/ASME/SAE/ASEE Joint Propulsion Conference, July 1-3, 1996, Lake Buena Vista, Florida.
11. Burggraf, O.R.: "Analytical and Numerical Studies of the Structure of Steady Separated Flows", Journal of Fluid Mechanics, Vol. 24, part 1, pp. 113-151, 1966.
12. Schallhorn, P.A. and Majumdar, A. K.: "Numerical Prediction of Pressure Distribution Along the Front and Back Face of a Rotating Disc With and Without Blades," AIAA 97-3098, Presented at the 33rd Joint Propulsion Conference, Seattle, Washington, July 6-9, 1997